

Development and Beam Irradiation of Ir/W/Ta/Ta-Alloys Refractory Metals and Cladding Via Hot Isostatic Pressing at CERN for Beam Intercepting Devices Applications

Josep BUSOM DESCARREGA¹, Claudio TORREGROSA¹ and Marco CALVIANI^{1*}

¹European Laboratory for Particle Physics (CERN), 1201 Geneva, Switzerland

*E-mail: marco.calviani@cern.ch

(Received: November 3, 2019)

The current contribution details the research and development activities associated to refractory metals such as iridium, tungsten, tantalum and tantalum-tungsten alloys executed at CERN in the framework of the development of beam intercepting devices, including beam irradiation tests both at the HiRadMat Facility as well as in the North Area Target Complex.

KEYWORDS: AD-target, Beam Dump Facility, BDF, iridium, tantalum, cladding, tungsten, hot isostatic pressing, dynamic behavior, HiRadMat

1. Introduction

The development of advanced materials and production techniques for CERN's beam intercepting devices is an ongoing activity at CERN. In particular, refractory metals are subject of specific attention for their excellent performance at high temperature and for their reduced nuclear inelastic scattering length, which is of particular importance for some physics cases.

The current contribution will detail specific studies and development for the production of a next generation antiproton production target at the Antiproton Decelerator (AD) facility, as well as studies aiming and validating the feasibility of the Beam Dump Facility production targets. For the former, summaries of a series of experiment conducted at the HiRadMat facility [1] are presented, while for the latter an overview of the cladding studies via hot isostatic pressing as well as the summary of a beam irradiation with slow extracted beams on a prototype target are described.

2. Antiproton production target: performances of refractory materials subjected to extreme dynamic stresses

The antiproton production target (AD-Target) at CERN requires a core made of a metal with the highest possible density and melting point. The objective is to have a very compact target in order to avoid antiproton reabsorption and to be as close as possible to a punctual source for the downstream collection and focusing of antiprotons. The proton beam impacting on the antiproton production target is composed by 4 proton bunches spaced by 105 ns, bunch length of 30 ns for a total pulse intensity of 1.5×10^{13} protons per

pulse. The total energy deposited in the target core is approximately 1.34 kJ, which results in 11.17 GW considering that it is deposited only in 120 ns. Moreover, the power is applied in a small volume of the target core, producing a mean power density of $2.87 \times 10^4 \text{ TW/m}^3$.

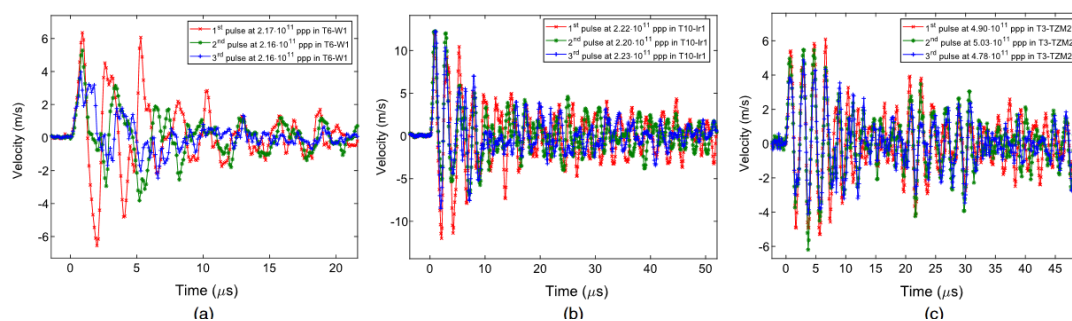


Fig. 1: Progressive distortion of the radial wave at these conditions suggests the appearance of internal cracks in these materials.

For this purpose, the target core design is based on rods of 2-10 millimeters in diameter by 5 cm in length made by a refractory metal such as iridium. The 26 GeV/c proton beam impacts on the core material during operation expose it to sudden rises of temperature close to 2000 °C within 0.5 μs, with subsequent dynamic stresses in the order of GPa, well above the core material's strength.

Extensive studies of the response of refractory metals at such conditions have been carried out over the last few years (2014-2018) at CERN motivated by the manufacturing of a new set of targets to guarantee future operation. It is believed that fracture of the target core due to beam induced dynamic loading is one of the main causes of the drop of antiproton yield observed during operation, probably due to a loss of effective density. Consequently, the primary goal of these studies was to improve the state-of-the-art of simulations used to understand the response of the target core at the extreme dynamic conditions of the AD-Target core. The approach consisted in using hydrocodes to simulate its dynamic response every time is impacted by the primary proton beam. This numerical tool allows the use of material strength models to simulate the material behavior beyond plastic deformation as well as failure models to take into account its potential fragmentation. In this context, a mechanical characterization at high temperatures (up to 1250 °C) and high strains rates (up to 10^4 s^{-1}) was performed to extract the parameters of such strength models for tungsten and iridium by means of Hopkinson bar tests [2][3].

The results of the hydrocode simulations indicated that a dominant radial vibration mode is excited in the target core as consequence of each of the 0.5 μs duration proton pulse impacts. This mode is excited due to the fact that most of the transversal area of the 3 mm diameter core is suddenly heated in a time that coincides with half of the period of the natural radial mode of vibration, leading to a constructive amplification that results in oscillating stresses from compression to tension at the core center [4].

In parallel to the numerical simulations, a set of experiments were performed to test refractory metals under real high-energy and intense proton beam impacts using the CERN's HiRadMat facility [1]. First of these tests was the HRMT-27 experiment, executed in 2015 [5]. The goal of this test was to assess the response of different refractory metals -possible candidates for the future material core such as tungsten, tungsten-

Lanthanum-doped, molybdenum, TZM-alloy (Mo alloy with 0.5 wt% titanium, 0.08 wt% zirconium and 0.03 wt% carbon), iridium and tantalum- at equivalent conditions as the ones reached in the AD-Target. The experimental targets were rods of 8 mm in diameter by 140 mm in length, which were impacted by 440 GeV/c proton beams through its longitudinal axis. Extensive online instrumentation was used to record the surface velocity during 500 ms after each impact. These measurements - presented in Fig.1 - were cross-checked with the hydrocode simulation predictions in order to validate the strength models used [6]. In addition, the measurements confirmed that the main damaging process is the excitation of the radial mode of vibration. Furthermore, other vibration modes excited by the proton beam impacts were also recorded (longitudinal and bending) and compared with simulation predictions [7]. The other main result of the experiment was that most of the tested materials showed extensive fracture at AD-Target conditions except tantalum, which mostly exhibited extensive plastic deformation. The recorded velocity at time of fracture was used to benchmark failure models for tungsten and iridium [6]. The greater response of tantalum with respect the rest of refractory metals encouraged its use a possible material alternative to iridium.

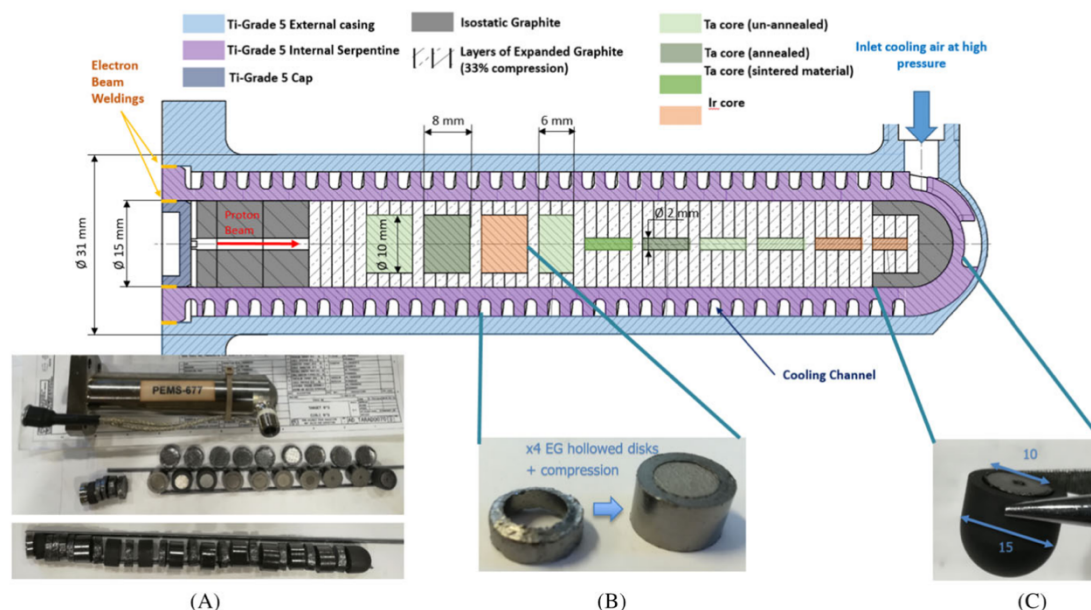


Fig. 2. The figure shows the schematics and photos of one of the HRMT48 experiments, showing the first real scale antiproton targets that will be operating from 2021 at CERN. This specific target is equipped with an EG matrix and cores of different diameters and grades of Ta and Ir (extracted from [10]).

The second HiRadMat test performed was the HRMT-42 experiment, executed in 2017 [8]. In this test, a target made of ten rods of tantalum with 8 mm in diameter embedded in a flexible graphite matrix and encapsulated in a Ti-6Al-4V container was exposed to 47 proton pulse impacts, recreating AD-Target conditions in each of them. The goal of this experiment was to test a scaled prototype of a potential new target design and to assess the behavior of tantalum when exposed to successive plastic deformation consequence of every proton beam impact. Post irradiation examinations of this target

revealed the creation of voids in the Ta material (ranging from 2 μm to 1 mm in diameter) induced by the proton beam impacts. The creation of such voids is identified as a consequence of the dynamic process of spalling, taking place under certain particularities, such as high temperature and cyclic loading, which are inherent to the unique load characteristics achieved by the proton beams. Detailed analysis of the observed voids and cross checks with simulations have been used to identify certain temperatures and pressure windows in which the growth of spalling voids seems to be enhanced [9].

Finally, the third HiRadMat test performed was the HRMT-48 PROTAD experiment, executed in 2018. In this experiment, up to six prototypes of the new AD-Target design (similar as the ones shown in Fig. 2) have been exposed to fifty proton beam impacts recreating AD-Target operation conditions [10]. The goal was to perform an integral testing of the new target design (which includes an air-cooled external assembly) as well as to validate the final core material selection. For this purpose, each of the targets was equipped with a different core configuration with multiple rods diameters (from 2 mm to 10 mm) and including different grades of tantalum, Ta2.5W, iridium, and tungsten doped with TiC. Neutron tomographies are then used to characterize the beam induced damage in such materials and the appearance of spalling voids.

3. Beam Dump Facility: application of hot isostatic pressing (HIP) technology to diffusion bond refractory metals for proton targets and absorbers

3.1 Introduction

In the framework of the Physics Beyond Colliders (PBC) initiative at the European Laboratory for Particle Physics (CERN), a new infrastructure named Beam Dump Facility (BDF) has been proposed to study the Hidden Sector.

The actual BDF production target design, shown in Figure 3, consists of several TZM and tungsten (W) cylinders with a diameter of 250 mm and variable lengths, for a total effective target length of 1.3 m. The target will require active water cooling to dissipate the deposited power. A detailed explanation of the target design is available in [11].

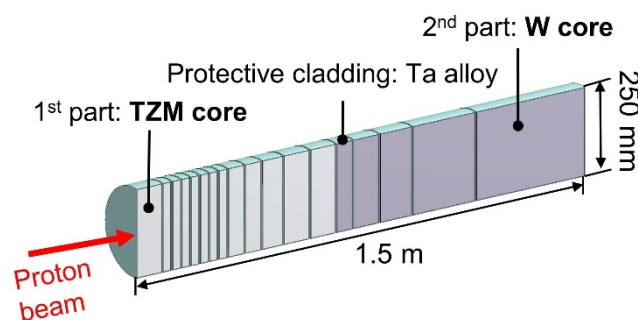


Fig. 3. 3D cross-sectional cut view of the BDF final target design, showing the TZM part as well as the W one, both clad with a Ta-alloy. The proton beam energy is 400 GeV/c.

For both target materials, multi-directionally forged material is required due to the stringent thermo-mechanical field but the available dimensions for this material grade are

limited. Thus, it was considered to diffusion-bond co-axially several multi-directionally forged cylinders.

W and TZM feature limited corrosion resistance in high temperature flowing water combined with irradiation conditions. Hence, the target blocks are covered with a 1 mm – 2 mm thick cladding. Ta and Ta2.5W are considered as cladding material for the suitable erosion-corrosion resistance and the extensive experience in other facilities. The most promising technique to diffusion bond the cladding to the target materials is Hot Isostatic Pressing (HIP) assisted diffusion bonding.

This work copes with multiple objectives. First, to explore for the first time the HIP assisted diffusion bonding between several target material cylinders (W to W and TZM to TZM). Second, to validate the HIP assisted diffusion bonding between all the cladding and target candidate materials for BDF, especially for the TZM and Ta2.5W, where no studies are reported. This study is specifically addressed to the diffusion bonded interfaces, since preparation routine was optimized in previous internal studies and no surface-related problems are encountered in this work. Details about the process are reported extensively in Ref. [12] together with the relevant references.

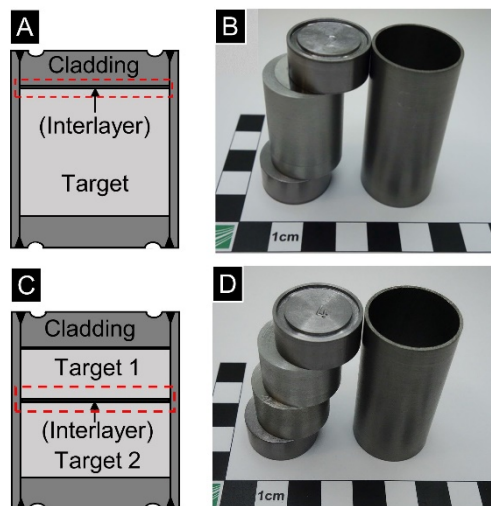


Fig. 4. Specimens' description and results of the interface SEM observation, tensile strength and thermal conductivity measurements.

3.2 Experimental

Several prototypes were fabricated to study the HIP assisted diffusion bonded interfaces. Four materials were employed in the fabrication of the prototypes, W and TZM as target materials, and Ta and Ta2.5W as cladding materials.

The prototypes were built using one or two cylinders of the target material. The cylinders were fitted inside a tube of cladding material and closed from the two sides by two covers, also from cladding material. The cladding material's thickness was of 1.5 mm in the cylindrical part, but it was increased to 10 mm for the two covers to allow the extraction of bigger bonding specimens, required for mechanical testing.

Two types of prototypes were built, either to study the target to cladding materials

bonding (see Figure 4A-B) or to study the target to target materials bonding (see Figure 4C-D). 50 μm thick Ta foils were eventually introduced between the materials as diffusion interfacial aids.

W was supplied by Plansee in form of both forged and annealed 25 mm and 50 mm diameter rods, with a minimal density of 99.97 % and a hardness of 420 HV – 480 HV. TZM was also supplied by Plansee in form of forged and annealed 25 mm - 50 mm diameter rods, with a hardness of 250 HV - 310 HV. Ta and Ta2.5W were supplied by Plansee and WHS Sondermetalle respectively, all products in the annealed state. The different diameters were requested in order to optimize the experimental setup. All the materials employed in this study did not undergo further specific surface preparation than conventional machining.

Before the HIP cycle, electron beam welding was employed to weld the tube and both covers of each prototype. The HIP cycle was carried out on the prototypes to diffusion bond the cladding material to the target material and eventually the target to target materials too. A HIP furnace with high purity Argon as pressurised gas and a Mo heater were employed. Additionally, the prototypes were wrapped with Ta and Zr foils to capture all the remaining impurities.

The heating rate during the HIP cycle was of 10 K/min and the dwell time at the nominal temperature and pressure was 3 hours. In this work, two HIP cycle parameters were tested: 1200 °C and 150 MPa (referred as "L") and 1400 °C and 200 MPa (referred as "H").

After the HIP cycle, Electro Discharge Machining (EDM) was employed to extract interface specimens from the prototypes. Metallographic preparation was carried out to allow interface imaging. Interface micrographs were acquired employing a Scanning Electron Microscope (SEM) Zeiss EVO 50 XVP with an accelerating voltage of 15 kV, a current of 300 pA and an operating distance of 8 mm.

Tensile testing was carried out on non-standard miniaturized tensile specimens of 4 mm² squared section. Testing was carried out employing a tensile testing Zwick 1476 system and a speed of 0.07 mm/min. Hardness measurements were carried out employing a Falcon 500 system from INNOVATEST with a Vickers indenter and a load of 5 N (HV5).

The thermal conductivity was calculated from the thermal diffusivity, measured using Xenon pyrometry "Nanoflash" from Netzsch, and the C_p , measured using "DSC204 Phoenix" from Netzsch.

3.3 Results and discussion

The results of the interfaces SEM observation, tensile strength and thermal conductivity measurements are summarized in Table 1. Successful bonding was accomplished for all the target to target material combinations but only when using interfacial aids (Ta interlayer). In these cases, interface microscopy revealed homogeneous and defect-free interfaces.

High quality bondings were achieved at the W/W and TZM/TZM interfaces, featuring tensile strengths of 215 MPa and 550 MPa respectively and negligible interface thermal resistance.

The HIP parameters did not show significant effects on the bondings. Nevertheless, the use of interfacial aids did show a significant strengthening effect in the mechanical strength of the bonding e.g. the strength of the TZM/TZM joint increased from 5 MPa to

550 MPa, even exceeding the strength of the interlayer material (220 MPa).

Successful bonding was also achieved between all the combinations of target materials (TZM and W) and cladding materials (Ta and Ta2.5W) and only some difficulties were encountered when bonding W and Ta2.5W with HIP cycle "L". Apart from the latter exception, all the interfaces showed homogeneous morphology without relevant defects. Diffusion layers with a thickness of approximately 1 μm could eventually be measured, in agreement with literature predictions.

Bonding specimen number	Target to cladding				Interface quality (from micrographs)	Interface tensile strength (% respect to cladding strength)	Interface thermal conductivity (% respect to theoretical)
	Target material	Cladding material	Interlayer	HIP			
1	TZM	Ta2.5W	x	L	Good	81	100
2		-	-		Good	70	90
3		Ta	-		Good	100	100
4	W	Ta2.5W	x	L	Good	67	89
5		-	-		No bonding	0	0
6		Ta	-		Good	85	94
7	TZM	Ta2.5W	x	H	Good	90	71
8		-	-		Good	90	100
9		Ta	-		Good	95	93
10	W	Ta2.5W	x	H	Good	54	99
11		-	-		Good	55	100
12		Ta	-		Good	71	100
Target to target							
	Target material 1	Target material 2	Interlayer	HIP		Interface tensile strength (MPa)	
13	TZM	TZM	-	L	Poor	5	100
14			Good		550	100	
15	W	W	-	L	No bonding	0	0
16			Good		220	93	
17	TZM	TZM	x	H	Good	470	100
18	W	W	x	H	Good	210	95

Table 1. A) Cross-sectional schematic of the prototypes designed to study the target to cladding materials bonding, with the specimen extraction area outlined in red, B) Image of the target to cladding materials prototype components before assembly, C) Cross-sectional schematic of prototypes designed to study the target to target materials bonding, with the specimen extraction area outlined in red and D) Image of the target to target materials prototype components before assembly

Ta provided satisfactory results as a cladding material, with either TZM or W as target materials, indicating complete diffusion bonding: almost 100 % joint efficiency and negligible interface thermal resistance were achieved.

The diffusion bonding of Ta2.5W to TZM was successful in all the cases, obtaining 100 % joint efficiency and negligible interface thermal resistance. Nevertheless, Ta2.5W required the use either higher temperature and pressure HIP parameters (cycle "H") or the addition of a Ta interlayer to achieve diffusion bonding with W. The difficulties to bond directly W to Ta2.5W could be attributed to the higher strength of the Ta2.5W compared to Ta or the drop of the diffusion rate due to the small concentration of W in the Ta.

Contrary to the target to target materials bonding, the HIP cycle parameters clearly affected the bonding properties. With Ta2.5W as a cladding material, using higher T and P (cycle "H") was beneficial to either initiate the bonding or to increase its mechanical strength. Contrarily, with Ta as a cladding material using higher T and P (cycle "H") lowered the interfacial strength, most probably due to the bulk materials' softening.

In both types of bonding (cladding to target materials and target to target materials) it

was found that incipient diffusion bonding is enough to remove the interface's thermal resistance. However, tensile strength of the joints resulted in being more sensitive, hence more indicated to assess the diffusion bonding extent.

3.4 Study conclusions

The building of a target block from several target material cylinders bonded together inside the Ta based cladding was validated. Diffusion bonding assisted by HIP was explored for the first time to self-bond W to W and TZM to TZM down-scaled target material cylinders, with promising results. Homogeneous and defect-free interfaces, bonding strengths of 550 MPa and 215 MPa (for TZM-TZM and W-W respectively) and negligible interface thermal resistance were achieved.

HIP was also proven to be a valid technique to diffusion bond the BDF candidate target materials (W and TZM) to Ta based erosion-corrosion resistant claddings (Ta and Ta2.5W) in cylindrical geometries representative of the final target. The reported experience in literature was limited to Ta clad W, but in this study, bondings with homogeneous interfaces, 100 % joint efficiency and negligible interface thermal resistances were achieved in the combinations Ta-TZM, Ta-W and Ta2.5W-TZM. The same was valid for the combination Ta2.5W-W only with a slightly lower joint efficiency of 70 %.

3.5 Prototype target beam test

In order to evaluate the response of the clad refractory metals to beam irradiation, an experimental setup was conceived built and operated in the North Area at CERN during 2018. The target consisted in a reduced scale BDF target composed by the same target core geometry with the exception of the diameter, which was reduced from 250 mm diameter to 80 mm diameter. Three days of beam time have been dedicated to the prototype test irradiation.



Fig. 5. Photos of the target prototype assembly being prepared for final installation. The right part shows the internal cladded blocks with the gaps between each other corresponding to a 5 mm gap required for the water cooling of the target assembly.

A total of 2.5×10^{16} protons on target has been sent to the spallation device, which was

also instrumented with temperature and strain gauges, in order to compare the simulations with the experimental results. The outcome of the comparison showed excellent agreement (within 10%) with simulations. Results are extensively reported in Ref. [13].

The next steps include a Post Irradiation Examination (PIE) studies of the spallation target, which will take place during 2020.

4. Conclusion

CERN has embarked into a project-driven study and application of refractory metals for beam intercepting devices, especially for target and dumps/absorbers. The endeavor includes high strain rate material studies, especially for iridium, pure tungsten and tantalum, beam irradiation with fast extracted pulses at the HiRadMat facility as well as cladding R&D via Hot Isostatic Pressing (HIP) and irradiation with slow extracted beams in the North Area target zone.

Acknowledgment

The authors would like to acknowledge the support from the Accelerator Consolidation Project, of the Beam Dump Facility study team within the Physics Beyond Collider studies as well as the EN-STI and EN-MME groups.

References

- [1] I. Efthymiopoulos et al., *Proc. 3rd Int. Particle Accelerator Conf. (IPAC'11)*, San Sebastian, Spain, 2011, pp. 1665–1667.
- [2] M. Scapin et al., *Int. Journ. Impc. Engin.* **106** (2017) pp 191-201.
- [3] M. Scapin et al., *Journ. Dyn. Behav. Mat.* **5-3** (2019) pp 296–308.
- [4] C. Torregrosa et al., *Phys. Rev. Accel. Beams* **19**, 073402.
- [5] C. Torregrosa et al., *Phys. Rev. Accel. Beams* **22**, 013401
- [6] C. Torregrosa, Universidad Politecnica de Valencia, March 2018 (CERN-THESIS-2017-357).
- [7] N. Solieri, Pisa University, December 2017 (CERN-THESIS-2017-340).
- [8] C. Torregrosa et al., *Phys. Rev. Accel. Beams* **21**, 073001
- [9] C. Torregrosa et al., Submitted to *International Journal of Solids and Structures*
- [10] C. Torregrosa et al., *Mat Design Process Comm.* 2019; **1**:e38. (<https://doi.org/10.1002/mdp2.38>).
- [11] E. Lopez Sola, M. Calviani et al., [arXiv:1904.03074](https://arxiv.org/abs/1904.03074), accepted in *Phys. Rev. Accel. Beams*
- [12] Busom Descarrega, J., Calviani, et al., T., *Mat Design Process Comm.* 2019; **1**–11. <https://doi.org/10.1002/mdp2.101> .
- [13] E. Lopez Sola, M. Calviani et al., [arXiv:1909.07094](https://arxiv.org/abs/1909.07094), submitted to *Phys. Rev. Accel. Beams*